

A New Lake Classification System based on Thermal Profiles to Better Understand the Most Dominant Lake Type on Earth

Bernard Yang¹, Mathew Wells², Bailey McMeans³, Hilary A. Dugan⁴, James A. Rusak⁵, Gesa A Weyhenmeyer⁶, Jennifer A. Brentrup⁷, Allison R. Hrycik⁸, Alo Laas⁹, Rachel M Pilla¹⁰, Jay A. Austin¹¹, Paul Blanchfield¹², Cayelan Carey¹³, Matthew M Guzzo¹⁴, Noah R Lottig¹⁵, Murray Mackay¹⁶, Trevor A. Middel¹⁷, Don Pierson¹⁸, Junbo Wang¹⁹, and Joelle Young²⁰

¹Department of Physical and Environmental Sciences, University of Toronto Scarborough, Toronto, Ontario, Canada

²Univeristy of Toronto

³University of Toronto - Mississauga

⁴University of Wisconsin–Madison

⁵Ontario Ministry of the Environment and Climate Change

⁶Ecology and Genetics/Limnology

⁷Department of Biology and Environmental Studies, St. Olaf College, Northfield, Minnesota, USA

⁸Rubenstein Ecosystem Science Laboratory, University of Vermont, Vermont, USA

⁹Estonian University of Life Sciences

¹⁰Miami University

¹¹University of Minnesota

¹²Department of Biology, Queen’s Univeristy

¹³Virginia Tech

¹⁴University of Guelph

¹⁵University of Wisconsin-Madison

¹⁶Environment Canada

¹⁷Harkness Laboratory of Fisheries Research, Aquatic Research and Monitoring Section, Ontario Ministry of Natural Resources, Trent University, Peterborough, Ontario, Canada

¹⁸Uppsala University

¹⁹Institute of Tibetan Plateau Research, Chinese Academy of Sciences

²⁰Environmental Monitoring and Reporting Branch

November 22, 2022

Abstract

Lakes are traditionally classified based on their thermal regime and trophic status. While this classification adequately captures many lakes, it is not sufficient to understand seasonally ice-covered lakes, the most common lake type on Earth. Here, we propose an additional classification to differentiate under-ice stratification. When ice forms in smaller and deeper lakes, inverse stratification will form with a thin buoyant layer of cold water (near 0°C) below the ice, which remains above a deeper 4°C layer. In contrast, the entire water column can cool to ~0°C in larger and shallower lakes. We suggest these alternative conditions for

dimictic lakes be termed “cryostratified” and “cryomictic.” We describe the inverse thermal stratification in 19 highly varying lakes and derive a model that predicts the temperature profile as a function of wind stress, area, and depth. The model opens up for a more precise prediction of lake responses to a warming climate.

A New Lake Classification System based on Thermal Profiles to Better Understand the Most Dominant Lake Type on Earth

Bernard Yang^{1*}, Mathew G. Wells^{1*}, Bailey C. McMeans², Hilary A. Dugan³, James A. Rusak^{4,5}, Gesa A. Weyhenmeyer⁶, Jennifer A. Bretrup^{7,8}, Allison R. Hrycik^{7,9}, Alo Laas¹⁰, Rachel M. Pilla¹¹, Jay A. Austin^{12,13}, Paul J. Blanchfield^{5,14}, Cayelan C. Carey¹⁵, Matthew M. Guzzo^{2,16}, Noah R. Lottig¹⁷, Murray D. Mackay¹⁸, Trevor A. Middel¹⁹, Don C. Pierson⁶, Junbo Wang²⁰, Joelle D. Young²¹

¹ Department of Physical and Environmental Sciences, University of Toronto Scarborough, Toronto, Ontario, Canada

² Department of Biology, University of Toronto Mississauga, Mississauga, Ontario, Canada

³ Center for Limnology, University of Wisconsin-Madison, Wisconsin, USA

⁴ Dorset Environmental Science Centre, Ontario Ministry of the Environment, Conservation, and Parks, Dorset, Ontario, Canada

⁵ Department of Biology, Queen's University, Kingston, Ontario, Canada

⁶ Department of Ecology and Genetics/Limnology, Uppsala University, Uppsala, Sweden

⁷ Rubenstein Ecosystem Science Laboratory, University of Vermont, Vermont, USA

⁸ Department of Biology and Environmental Studies, St. Olaf College, Minnesota, USA

⁹ Department of Biology, University of Vermont, Vermont, USA

¹⁰ Chair of Hydrobiology and Fishery, Institute of Agricultural and Environmental Sciences, Estonian University of Life Sciences, Tartu, Estonia

¹¹ Department of Biology, Miami University, Oxford, Ohio, USA

¹² Large Lakes Observatory, University of Minnesota Duluth, Duluth, Minnesota, USA

¹³ Department of Physics and Astronomy, University of Minnesota Duluth, Duluth, Minnesota, USA

¹⁴ Fisheries and Oceans Canada, Winnipeg, Manitoba, Canada

¹⁵ Department of Biological Sciences, Virginia Tech, Blacksburg, Virginia, USA

¹⁶ Department of Integrative Biology, University of Guelph, Guelph, Ontario, Canada

¹⁷ Center for Limnology Trout Lake Station, University of Wisconsin-Madison, Wisconsin, USA

¹⁸ Environmental Numerical Weather Prediction Research, Science and Technology Branch, Environment and Climate Change Canada, Canada

¹⁹ Harkness Laboratory of Fisheries Research, Aquatic Research and Monitoring Section, Ontario Ministry of Natural Resources, Trent University, Peterborough, Ontario, Canada

²⁰ Key Laboratory of Tibetan Environment Changes and Land Surface Processes (TEL) / Nam Co Observation and Research Station (NAMORS), Institute of Tibetan Plateau Research, Chinese Academy of Sciences, Beijing 100101, China

²¹ Ontario Ministry of the Environment, Conservation, and Parks, Toronto, Ontario, Canada

*Corresponding authors: Bernard Yang (bernie.yang@utoronto.ca), Mathew Wells

(m.wells@utoronto.ca)

Key points

- Standard classifications of dimictic lakes do not consider how variable the initial thermal stratification can be under winter lake ice

46
47
48
49
50
51

- Lakes that are shallow or windy can cool to near 0-1°C before ice forms and are weakly stratified, which we term “cryomictic”
- Deeper lakes or those with calmer winds, result in ice forming just above deeper waters of 3-4°C, which we term “cryostratified”

52
53
54
55
56
57
58
59
60
61
62
63
64
65
66
67

Author Contribution Statement: This project was initiated in a workshop at the 21st Global Lakes Ecological Observatory Network meeting in Huntsville, Ontario, Canada in 2019. The authors are listed in four groups: BY-BCM; HAD-GAW; JAB-RMP; and JAA-JDY. The first group is listed in order of contribution in writing the manuscript. The second group, listed alphabetically, includes authors who attended the workshop, and participated in the initial framing for the project, and were involved in designing the structure of the manuscript. The third group, listed alphabetically, attended the workshop and participated in the initial framing for the project. The fourth group, listed alphabetically, prepared data for the analysis and contributed feedback. The specific contributions are as follows: BY and MGW conceived the idea for the manuscript and coordinated the project. HAD, ARH, AL, RMP, GAW, MGW, and BY participated at the initial project discussion during the meeting. BY conducted the data analysis and prepared the figures. HAD, JAR, GAW, MGW, and BY designed the manuscript. BY wrote the manuscript under the supervision of MGW. BCM wrote the section on biological influences. JAA, JAB, PJB, CCC, HAD, MMG, ARH, AL, NRL, MDM, TAM, DCP, RMP, JAR, JW, MGW, BY, and JDY prepared the data for the analysis. All authors provided critical feedbacks and approved the manuscript.

68
69

Abstract

70
71
72
73
74
75
76
77
78
79
80
81
82

Lakes are traditionally classified based on their thermal regime and trophic status. While this classification adequately captures many lakes, it is not sufficient to understand seasonally ice-covered lakes, the most common lake type on Earth. Here, we propose an additional classification to differentiate under-ice stratification. When ice forms in smaller and deeper lakes, inverse stratification will form with a thin buoyant layer of cold water (near 0°C) below the ice, which remains above a deeper 4°C layer. In contrast, the entire water column can cool to ~0°C in larger and shallower lakes. We suggest these alternative conditions for dimictic lakes be termed “cryostratified” and “cryomictic.” We describe the inverse thermal stratification in 19 highly varying lakes and derive a model that predicts the temperature profile as a function of wind stress, area, and depth. The model opens up for a more precise prediction of lake responses to a warming climate.

83
84
85

Plain Language Summary

86
87
88
89
90
91

Most mid and high latitude lakes are seasonally ice-covered and have only been classified based on the thermal structure and trophic status during the open-water season in summer. However, limited temperatures observations in these ice-covered lakes suggest that there is a wide range of thermal structures over winter. We developed an analytical model to predict the average water temperature at the time of ice formation based on the strength of the surface winds, the area of

92 the lake, and the maximum depth of the lake. Using both the analytical model and water
 93 temperature data from 19 different lakes in North America, Europe, and Asia, we found that the
 94 time of ice formation in lakes that are large or experience strong winds were later compared to
 95 lakes that are small or experience weak winds. The larger and windier lakes are also generally
 96 colder (0~2°C) than smaller and calmer lakes (2~4°C) at the time of ice formation. This suggests
 97 that these seasonally ice-covered lakes can be subdivided into two additional classes during
 98 winter. The analytical model and the new classification have important consequences for
 99 understanding fish habitat under the ice and the potential effects of climate change on these
 100 seasonally ice-covered lakes.

103 Introduction

104
 105 At least 50% of the lakes in the world are located at high latitudes and are seasonally ice-covered
 106 (Verpoorter et al., 2014). Therefore, it is important to understand the broad controls on thermal
 107 stratification present during winter in these ubiquitous cold monomictic and dimictic lakes at
 108 temperate and boreal regions. In both types of lakes, the water column becomes thermally
 109 stratified under lake ice in the winter. While considerable effort has been made to describe the
 110 details and drivers of summer thermal stratification in dimictic lakes (e.g., Boehrer and Schultze,
 111 2008), most textbooks do not go much beyond saying that during winter an inverse stratification
 112 exists (e.g., Wetzel, 2001), following the original classification scheme of dimictic lakes by
 113 Lewis (1983). In the lake classification scheme given by Lewis (1983), only four examples of
 114 dimictic lakes are given, of which only 2 lakes (Lake Erken in Sweden and Lake Mendota in
 115 Wisconsin, USA) were not meromictic. It is unclear, however, to what degree these two lakes
 116 should be considered archetypes of winter conditions in *all* dimictic lakes. In particular, the
 117 strength of thermal stratification and mixing that occurs before and during ice formation remains
 118 unknown, as under-ice processes have been reported in only 2% of the peer-reviewed literature
 119 on freshwater systems (Hampton et al., 2015, 2017). Once ice onset occurs in dimictic lakes, the
 120 initial thermal stratification present during ice formation largely persists through the whole
 121 winter prior to the late-winter convection period (Bruesewitz et al. 2015; Yang et al., 2017, 2020;
 122 MacKay et al. 2017). The resulting under-ice thermal profile regulates biological activity, as both
 123 a habitat for fish (McMeans et al., 2020), plankton (Kelley, 1997, Hampton et al., 2015), and as a
 124 control on microbial processing. It also influences lake hydrodynamics, through control on
 125 internal waves, circulation and vertical mixing (Kirillin et al., 2012). Consequently, determining
 126 the drivers of under-ice thermal stratification in dimictic lakes is needed to better understand
 127 under-ice conditions as they rapidly change (Hampton et al., 2017), especially as lakes are
 128 warming under a changing climate (O'Reilly et al., 2015).

129
 130 The extent of surface mixing after the water column cools to 4°C and before ice forms in the fall
 131 or early winter controls the heat distribution through the water column, and thus influences the
 132 thermal stratification at ice-on (Figure 1). The mixing dynamics are determined by the non-linear
 133 equation of state, where freshwater becomes less dense as temperature decreases below 4°C.
 134 Thus, cooling that occurs above 4°C destabilizes the water-column, whereas when the water-
 135 column cools below 4°C there is a stabilizing buoyancy flux that restratifies the water column
 136 (Farmer and Carmack, 1981). In general, lakes subjected to more intense wind mixing during
 137 late fall will have lower water column temperatures, so that wind speed prior to ice formation

138 should determine early winter temperature profiles (Farmer and Carmack, 1981). Using the idea
 139 of a one-dimensional Monin-Obukhov scaling, Farmer and Carmack (1981) suggested that a
 140 vertical length scale for the cold buoyant layer is $H_{FC} \sim u_*^3/B$, where u_* is the friction velocity
 141 and B is the buoyancy flux per unit area. Hence stronger winds result in a deeper cold layer
 142 before ice-on (Figure 1a,1c), whereas calmer lakes have shallower cold surface layers (Figure
 143 1b,1d). The same balance between vertical mixing and a stable buoyancy flux applies to the
 144 summer thermocline, and a similar Monin-Obukhov scaling argument has been used by Kirillin
 145 and Shatwell (2016) to separate the summer stratification of 378 lakes into polymictic or
 146 stratified dimictic systems.

147
 148 The physics of inverse stratification prior to formation of ice cover is analogous to the widely
 149 studied process of thermocline formation in early summer in dimictic lakes. For instance, the
 150 depth of a dimictic lake's thermocline can also be related to the magnitude of wind-driven
 151 mixing and the lake's geometry. Gorham and Boyce (1989) used a two-dimensional argument
 152 based on the Wedderburn number to show that the depth of the late summer thermocline scaled
 153 as

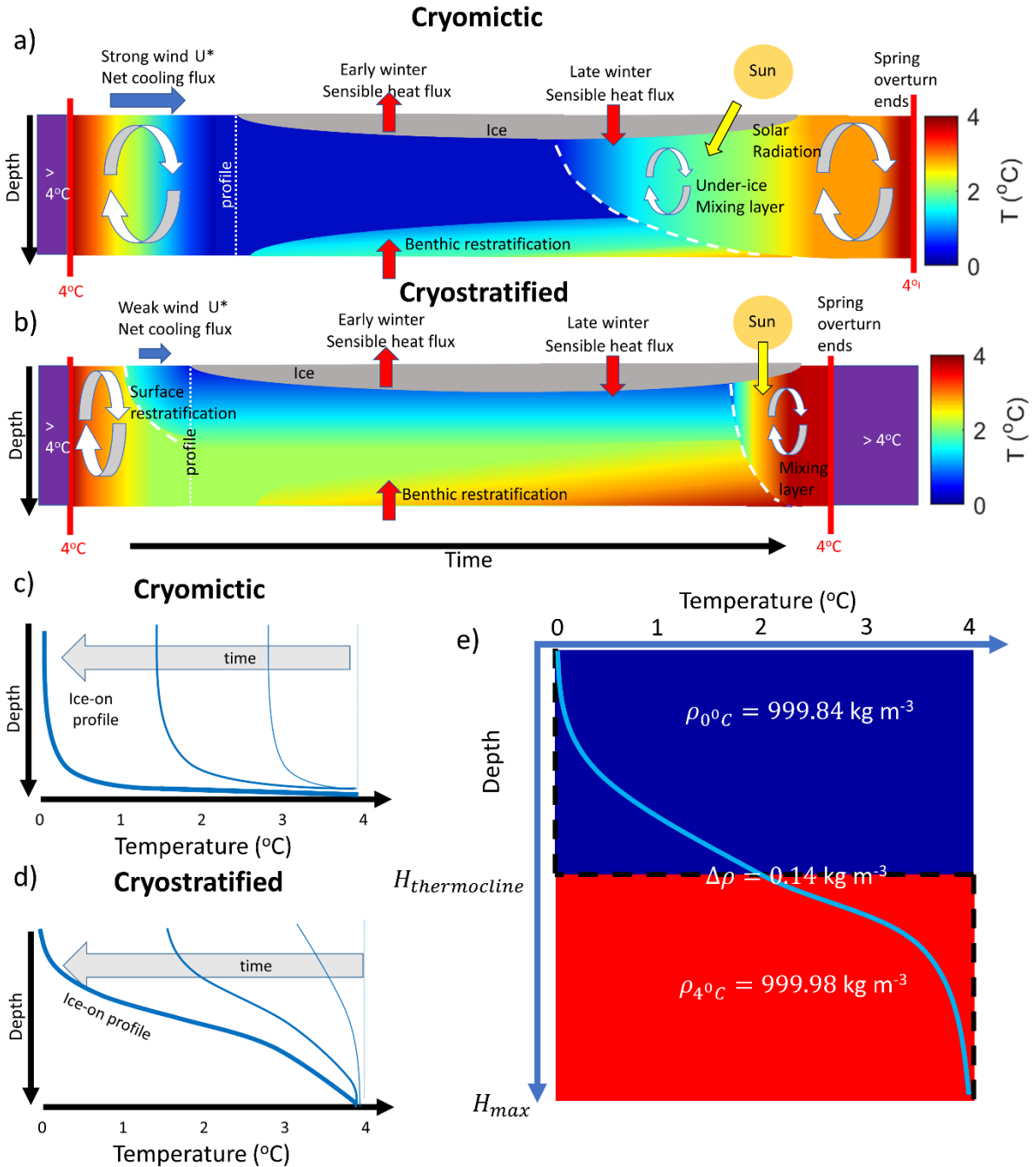
$$154 \quad H_{GB} \sim \bar{u}_* \sqrt{L/g'} \quad (1)$$

155
 156 where \bar{u}_* is the friction velocity averaged over the summer stratified period, L the fetch and g'
 157 the reduced gravity across the thermocline, defined as $g' = g \Delta\rho/\rho_o$, where g is the
 158 gravitational acceleration, $\Delta\rho$ is the density difference across the thermocline, and ρ_o is the
 159 average density of the water column. In contrast to the one-dimensional Monin-Obukhov scaling
 160 used by Farmer and Carmack (1981) and Kirillin and Shatwell (2016), this scaling explicitly
 161 includes the effects of the lake geometry, namely the fetch of the lake. Gorham and Boyce
 162 (1989) found a good agreement with their prediction when looking at end-of-summer
 163 thermocline depths H in 150 lakes. Fee et al. (1996) found that H during midsummer had a
 164 positive correlation with $A^{\frac{1}{4}}$, where A is the surface area of the lake. If the lake is circular, then
 165 $A^{\frac{1}{4}} \sim L^{\frac{1}{2}}$. For a fixed wind speed, this is the same scaling relationship as $H_{GB} \sim L^{\frac{1}{2}}$ obtained by
 166 Gorham and Boyce (1989). Both the one and two-dimensional arguments suggest that with more
 167 wind, the thermocline during the formation of stratification in a dimictic lake becomes deeper, a
 168 result that applies to both early summer and early winter. However, this scaling has never been
 169 applied to winter conditions before.

170
 171 Despite the extensive work published on quantifying the relative contributions of surface
 172 momentum flux to buoyancy flux in establishing the summer dynamics, there is no comparable
 173 work on the fall overturn period establishing the under-ice stratification. This idea has not been
 174 tested against a broad geographical suite of ice-covered lakes with differing depths, surface areas
 175 and wind speeds, likely because winter field work has substantial logistical challenges (Block et
 176 al., 2019). In this analysis, we use temperature and wind speed data from 19 lakes across North
 177 America, Europe, and Asia to explore the degree to which winter thermal stratification in ice-
 178 covered lakes is controlled by wind. Using these results, we suggest that the traditional
 179 classification by thermal regime and trophic status is not sufficient to understand the early winter
 180 stratification in dimictic lakes. We provide an additional classification for dimictic lakes based
 181 on the thermal stratification patterns across the different lakes in the study: *cryomictic* for lakes
 182

183 that are cold and mixed at ice-on, and *cryostratified* for lakes that are warmer and stratified at
 184 ice-on. This additional classification has broad implications for our understanding of under-ice
 185 conditions in dimictic lakes.

186
 187



188
 189 **Figure 1:** Schematic showing the difference in thermal structure between a) a wide, shallow, and
 190 windy lake with a deeper cold layer and weak stratification, and b) a small, deep, and calm lake
 191 with strong inverse stratification. Corresponding evolution of temperature profiles until ice-on

192 for c) wide lake and d) small lake. e) An idealized schematic of winter thermocline depth
 193 $H_{thermocline}$ used to develop our theory with the black dashed line showing the vertical
 194 temperature profile for the idealized two-layer model and the blue curve as an example of an
 195 actual vertical temperature profile.

196

197 **Study Sites and Data**

198

199 To analyze and classify the thermal profiles of lakes over a range of geographic locations with
 200 different climatic conditions, we used continuous water temperature measurements from 19 lakes
 201 across North America, Northern Europe, and Asia. This dataset covers a broad range of surface
 202 areas and maximum depths (Figure S1; Table S1). We defined the start of the inverse
 203 stratification period to be the time when the vertically averaged water temperature was 4°C, close
 204 to the temperature of maximum density of freshwater (Chen and Millero, 1986), and we defined
 205 the timing of ice-on to be the day of full ice cover. In larger lakes that are often partially ice-
 206 covered, we defined the timing of ice-on to be the first day where at least a radius of 10 km from
 207 the sampling point is ice-covered, which is consistent with the definition used in Titze and
 208 Austin (2016) (Table S1). In all lakes, water temperature was measured continuously at multiple
 209 depths (Table S1). The water temperature measurements were then extracted between the start of
 210 the inverse stratification period and the onset of ice-cover. Out of the 19 lakes in this study, 13
 211 lakes included hourly wind speed measurements near the surface of the lake. Detailed lake
 212 characteristics including the geographic location, mean depth, maximum depth, surface area, and
 213 sampling rates are given in Table S1.

214

215 **Calculating depth averaged temperatures**

216

217 The depth-averaged temperature T_{avg} was calculated at the time of reported ice-on. In many
 218 cases moorings did not extend to the surface, due to vulnerability of the instruments to the lake
 219 ice, and instead the shallowest thermistors were typically below ice at 0.5 to 2-m depth. In these
 220 cases, we assumed that $T = 0$ at $z = 0$, and made a linear interpolation between that and the
 221 highest measurement. We also assumed that the temperature at the bottom was equal to the
 222 temperature at the deepest logger. Typically, this represents a slight underestimation of the actual
 223 depth-averaged temperature due to the inverse thermal stratification in cold lakes. However,
 224 there are special cases where compressibility effects were significant in very deep lakes (e.g.
 225 Lake Superior), resulting in an overestimation of the depth-averaged temperature at ice-on.

226

227 **Calculating time averaged winds and the drag coefficient**

228

229 For each lake, we determined the average surface wind at 10 m above the surface of the lake,
 230 U_{10} , by averaging the wind speeds between the start of inverse stratification and onset of ice
 231 cover. In cases where the wind measurements were made at another height z , we used a power-
 232 law scaling formula to estimate U_{10} following Hsu et al (1994).

$$U_{10} = U_z \left(\frac{10}{z} \right)^{0.11}$$

233

234 where U_z is the wind measured at height z above the surface of the lake. To account for the
 235 variability of the wind measurements during this period, we calculated the sample standard

236 deviation of all the wind speeds to obtain the wind speeds at the 25th and 75th percentile that were
 237 used to construct the error bars.

238

239 The drag coefficient $C_{D,10}$ was calculated using Charnock's Law (Charnock, 1955) and the
 240 empirical relationship determined by Wüest and Lorke (2003)

241

$$C_{D,10} = \begin{cases} 0.0044U_{10}^{-1.15}, & U_{10} < 5 \text{ m s}^{-1} \\ \left[\kappa^{-1} \ln \left(\frac{10g}{C_{D,10}U_{10}^2} \right) + 11.3 \right]^{-2}, & U_{10} > 5 \text{ m s}^{-1} \end{cases}$$

242

243 where κ is the von Karman constant and g is the gravitational acceleration.

244

245 Modelling Approach

246

247 **Modelling the water temperature at ice formation based on wind measurements and** 248 **geometry of the lake**

249

250 The average temperature at ice-on can be estimated from a highly simplified two-layer model
 251 that has a top layer of thickness $H_{thermocline}$ and a total depth of H_{max} , where the temperature is
 252 set to 0°C above the winter thermocline and 4°C below (as sketched in Figure 1e). The depth
 253 averaged temperature of a lake at ice-on in degrees Celsius can be calculated as

254

$$T_{ice-on} = \frac{1}{H_{max}} (0 \times H_{thermocline} + 4 \times (H_{max} - H_{thermocline}))$$

255

256 which simplifies to

257

$$T_{avg} = 4 \left(1 - \frac{H_{thermocline}}{H_{max}} \right) \quad (2)$$

258

259 We define the depth of the thermocline based on the results of Gorham and Boyce (1989), who
 260 modelled the full scaling of the thermocline depth based on wind driven mixing events as

261

$$H_{thermocline} \equiv H_{GB} = 2 \left(\frac{\tau}{g\Delta\rho} \right)^{\frac{1}{2}} A^{\frac{1}{4}} \quad (3)$$

262

263 where τ is the surface wind stress, A is the surface area of the lake, and $\Delta\rho$ is the density
 264 difference between the two layers. The surface wind stress is given by

265

$$\tau \equiv \rho_w u_*^2 = \rho_a C_{D,10} U_{10}^2 \quad (4)$$

266

267 where ρ_w is the density of water (taken to be 1000 kg m⁻³ here), ρ_a is the density of air (1 kg m⁻³),
 270 U_{10} is the wind speed measured 10 m above the surface of the lake, and $C_{D,10}$ is the drag
 271 coefficient for surface winds at 10 m. Hence the friction velocity

272

$$u_* = \sqrt{\frac{\rho_a}{\rho_w} C_D U_{10}^2} \quad (5)$$

274
275 The local wind stress experienced between nearby lakes can vary (Read et al., 2012), depending
276 upon local topography and the influence of wind sheltering (Markfort et al., 2010). Generally,
277 these effects mean that larger lakes have stronger winds (i.e. $u_* \sim L$), when compared to nearby
278 lakes of smaller area.

279
280 Combining equations 3–5, the depth of the thermocline can be written as
281

$$H_{thermocline} = 2 \left(\frac{\rho_a C_{D,10} U_{10}^2}{\rho_w g'} \right)^{\frac{1}{2}} A^{\frac{1}{4}} \quad (6)$$

283
284 where g' is the reduced gravity defined in terms of the density difference between 0 and 4°C
285 water as $g' = g (\rho_{4^{\circ}C} - \rho_{0^{\circ}C}) / 0.5(\rho_{4^{\circ}C} + \rho_{0^{\circ}C})$. Using this, we obtain a novel estimation of the
286 depth-averaged temperature at ice-on based on both the surface winds over the lake and the
287 geometry of the lake by substituting into equation 1
288

$$\hat{T}_{ice-on} = \max \left\{ 0, 4 \left(1 - \frac{2 \rho_a^{\frac{1}{2}} \rho_w^{-\frac{1}{2}} C_{D,10}^{\frac{1}{2}} g'^{-\frac{1}{2}} U_{10} A^{\frac{1}{4}}}{H_{max}} \right) \right\} = \max \left\{ 0, 4 \left(1 - \frac{2 u_* g'^{-\frac{1}{2}} A^{\frac{1}{4}}}{H_{max}} \right) \right\} \quad (7)$$

289

290 **Results**

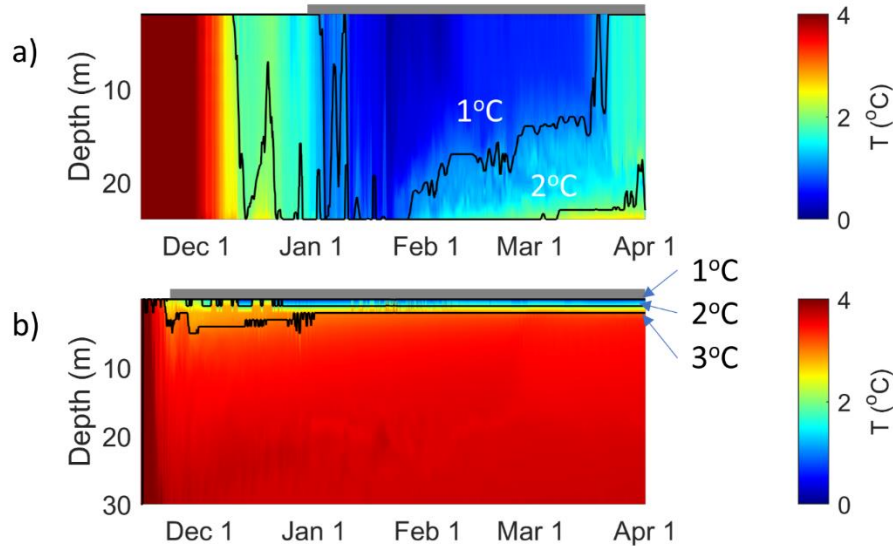
291

292 **Detailed comparison of thermal stratification during the fall and winter between a small** 293 **and large lake**

294

295 Our new modelling approach suggests that local wind and lake area have important roles in
296 determining the thermal profile at ice formation, and the extent to which dimictic lakes can vary
297 between being cryomictic and cryostratified. This difference in thermal profiles is seen most
298 clearly when comparing Lake Mendota (surface area 39.6 km²) with Harp Lake (surface area
299 0.714 km²). These lakes have similar maximum depths (25-30 m) and are at approximately the
300 same latitude (43-45 degN) in mid-continental North America, thus experience relatively similar
301 air temperatures and solar radiation. The most important difference between the lakes is the wind
302 they experience. The average wind U_{10} on Lake Mendota at the start of the inverse stratification
303 period and prior to ice-on was 5.8 m s⁻¹, much windier than the sheltered Harp Lake, where the
304 average U_{10} was only 0.9 m s⁻¹ prior to ice formation. Consequently, temperature profiles of the
305 two lakes at the time of initial ice formation were different, which influenced the stratification
306 pattern during winter. During the early winter of 2019 between ice-on and February 1 in Lake
307 Mendota, the water column was nearly isothermal. Before the surface-mixing layer started to
308 develop in late March, most of the upper water column remained close to isothermal. Beneath
309 the isothermal upper layer, the temperature was increasing at approximately 0.15°C m⁻¹, and the
310 strongest stratification was at the bottom of the lake where the temperature increased at 0.5°C m⁻¹.
311 In contrast, Harp Lake had only a thin surface layer near the surface that was less than 3°C. This
312 surface layer was less than 3-m thick and strongly stratified where the maximum temperature

313 gradients were $1.5^{\circ}\text{C m}^{-1}$. Beneath this strongly stratified layer, the water column was between 3
 314 and 4°C and the temperature gradients did not exceed $0.1^{\circ}\text{C m}^{-1}$.
 315



316 **Figure 2:** Difference in thermal structure between a) Lake Mendota (a large lake, 43.1°N), and
 317 b) Harp Lake (a small lake, 45.3°N) during the winter of 2019. These two lakes are at a similar
 318 latitude yet the thermal stratification in Lake Mendota was weak and colder compared to Harp
 319 Lake. While the Harp Lake site is 36-m deep, data are only shown for the top 30 m where
 320 continuous measurements were taken. In both plots, the gray bar on top of both plots indicate the
 321 duration of ice cover.
 322

323
 324 **Comparison of water temperature at ice-on with lake size and the strength of surface winds**
 325

326 Extending the observations to 19 lakes globally, our data shows that the ice-on temperature
 327 profiles vary widely (Figure 3a). Lake Erie had the coldest temperature at ice-on at nearly 0°C
 328 and was nearly isothermal. The temperature profiles in other larger lakes such as Lake Simcoe
 329 were less than 1°C in the upper half of the water column, and between 1°C and 2°C near the
 330 bottom of the lake. In contrast, in other smaller lakes such as Alexie Lake, the water column was
 331 generally $> 2^{\circ}\text{C}$ where the temperature near the bottom can be close to 4°C , the temperature of
 332 maximum density.
 333

334 We found a strong relationship between the surface winds and the depth-averaged ice-on
 335 temperatures. Lakes that experience weaker surface winds prior to ice-on had higher average
 336 temperatures at ice-on, while stronger winds led to lower average temperatures at ice-on (Figure
 337 3b). This is consistent with stronger winds driving a deeper surface mixing layer prior to ice-on
 338 that transports colder waters to the bottom. The ice-on temperatures of each lake also appear to
 339 be well-correlated to the geometry of the lake H_{mean}/\sqrt{A} , where A is the surface area of the lake.
 340 This value is high for small, deep lakes and low for large, shallow lakes (Figure 3c). In general,
 341 we found that a larger surface area of the lake corresponds to higher average strength of the

342 surface winds (Figure 3d). The temperature scaling using our new idealized two-layer model
343 (equation 7) agreed very well with the measured average temperature during ice-on (Figure 3e).

344

345

346

347

348

349

350

351

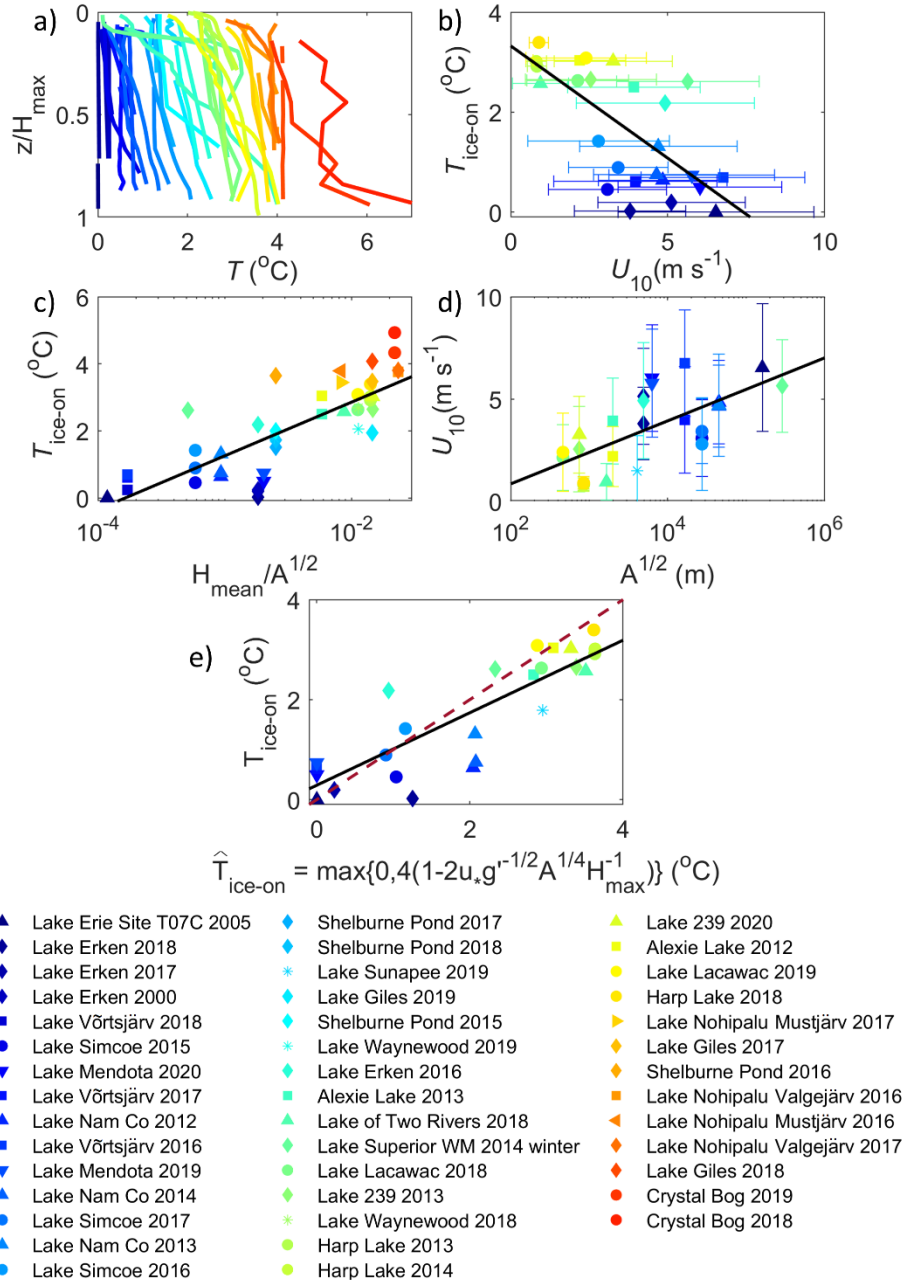
352

353

354

355

356



357
358
359

360 **Figure 3:** Water temperatures in our study lakes, each denoted by a unique color/symbol
 361 combination: a) Temperature profiles of each lake at ice-on with depth (z) on the y-axis
 362 normalized by the maximum depth of each lake (H_{\max}). b) Relationship between...Depth-
 363 averaged temperature at ice-on ($T_{\text{ice-on}}$) compared to $\overline{U_{10}}$, which, for lakes with wind data, was
 364 averaged from when the water column cooled to 4°C to ice-on. c) $T_{\text{ice-on}}$ compared to the ratio
 365 of the mean depth (H_{mean}) and the square root of the lake surface area ($A^{1/2}$). d) $\overline{U_{10}}$ during the
 366 same period in b) compared to $A^{1/2}$. e) Observed $T_{\text{ice-on}}$ compared to $\hat{T}_{\text{ice-on}}$ (modelled using

367 equation 7) with the dashed line representing 1:1. The black lines indicate the linear regressions
 368 for b) $T_{ice-on} = 3.32 - 0.45\bar{U}_{10}$, $R_{adj}^2 = 0.463$, slope $p < 0.01$, c) $T_{ice-on} = 6.32 +$
 369 $0.73 \log(H_{mean}A^{-1/2})$, $R_{adj}^2 = 0.672$, slope $p < 0.0001$, d) $\bar{U}_{10} = -2.23 + 0.67 \log(A^{1/2})$,
 370 $R_{adj}^2 = 0.43$, slope $p < 0.001$, and e) $T_{ice-on} = 0.29 + 0.73 \hat{T}_{ice-on}$, $R_{adj}^2 = 0.726$, intercept
 371 $p = 0.177$, slope $p < 0.001$. Red colours indicate warmer T_{ice-on} and blue colours indicate
 372 colder T_{ice-on} .
 373

374 Discussion

375
 376 Our synthesis of data from 19 lakes in North America, Europe, and Asia suggests that there is a
 377 large variation of ice-on temperature profiles that vary between cryomictic and cryostratified,
 378 and that mean ice-on temperatures were well-predicted by lake depth, fetch and wind stress prior
 379 to ice-on (equation 7). For lakes without available wind data, we found that the depth-averaged
 380 temperature at ice-on correlated well with $\log(H_{mean}/\sqrt{A})$, where larger values indicate a
 381 deeper lake relative to its surface area. We emphasize that although the correlation coefficients
 382 R_{adj}^2 are similar between comparing T_{ice-on} against $\log(H_{mean}/\sqrt{A})$ ($R_{adj}^2 = 0.672$, Figure 3c)
 383 and comparing T_{ice-on} against the two-layer model scaling ($R_{adj}^2 = 0.726$, equation 7, Figure
 384 3e), the new two-layer model scaling is based on the essential physics of the mixing layer depth
 385 proposed by Gorham and Boyce (1989) during wind events. However, if the friction velocity can
 386 be assumed to be an increasing function of \sqrt{A} (Figure 3d), then the two-layer model scaling
 387 (equation 7) suggests that T_{ice-on} will be a function of the vertical aspect ratio H_{mean}/\sqrt{A}
 388 (Figure 3c). Here, we found that most cryostratified lakes at ice-on have larger values of
 389 $\log(H_{mean}/\sqrt{A})$ and have weaker winds (Figure 3c).
 390

391 More generally, the data and equation (7) suggest that the initial under-ice winter thermal
 392 stratification of a dimictic lake is best characterized by a gradient - on one end the depth-
 393 averaged temperatures are “cold” and close to 0°C with near uniform temperatures in a weakly
 394 stratified lake, whereas at the other end, the lake is “warm” with a thin cold layer of water
 395 immediately beneath the ice and then a deep layer of water that is near 4°C. In light of this, we
 396 suggest that it is useful to further subdivide the dimictic classification scheme of Lewis (1983)
 397 into additional categories and that the term “*inverse stratification*”, when applied widely to
 398 characterize seasonally ice-covered lakes, may be misleading in many cases. We suggest that a
 399 new term of “*cryostratified*” lakes be used when the depth-averaged initial winter temperature is
 400 between 2–4°C under the ice (i.e. Harp Lake, Figure 2b), and the term “*cryomictic*” lakes be used
 401 where depth-averaged temperatures are between 0–2 °C (i.e. Lake Mendota, Figure 2a). In the
 402 absence of additional chemical stratification, all initial under-ice winter temperature profiles
 403 exist on a continuum between these states. The use of these new will be helpful when comparing
 404 different lakes with regard to biogeochemical processes, fish habitat usage over winter, or
 405 advancing our understanding of under-ice dynamics in lakes. Here, we provide two examples of
 406 its relevance for biological and physical processes in lakes.
 407

408 **Implications of the new classification system for biological processes**

409

410 The division of lakes into *cryostratified* and *cryomictic* may help to better understand the
 411 abundance of fish. Fish are ectotherms, so their use of different thermal habitat in a stratified
 412 water column has implications for their physiological rates and performance (Huey, 1991).
 413 Freshwater fish are known to select particular habitats that align with their thermal preferences
 414 (Brandt et al. 1980). However, much of this work has been restricted to open water periods. Fish
 415 habitat choice in winter, when temperatures range from near 0°C just below ice to temperatures
 416 as “warm” as 4°C at the bottom, is poorly understood. Both winter inactive (e.g. smallmouth
 417 bass, Suski and Ridgway, 2009) and winter active (e.g. burbot; Harrison et al., 2016) fish species
 418 appear to select for particular depths during winter, and a number of recent studies on salmonids
 419 suggest that these cold-adapted fish often occupy higher and colder regions of the water column
 420 in a narrow depth range during winter that corresponds to temperatures between 1–3°C
 421 (Blanchfield et al., 2009; McMeans et al., 2020; Bergstedt et al., 2003; Cote et al., 2020; Mulder
 422 et al., 2018; Gorsky et al., 2012). Although most ice-covered lakes have temperatures in the
 423 range 0–4°C, the degree of stratification can vary substantially between lakes. If fish are indeed
 424 choosing a specific 2°C isotherm, this layer would be deeper and potentially narrower in
 425 cryomictic lakes, versus cryostratified lakes. For instance, the 2°C isotherm is at approximately
 426 90% of lake depth in the colder Lake Mendota, versus approximately 5% depth in Harp Lake
 427 (Figure 2). The degree to which differing winter stratification patterns drive different depth usage
 428 by various fish, and the resultant consequences for fish growth and survival, would therefore be a
 429 valuable research topic for future telemetry studies.

430

431 **Implications of the new classification system for under-ice physical processes**

432

433 Initial differences in thermal stratification under the ice influence late winter stratification, and
 434 can subsequently influence the magnitude of two key physical processes, namely (1) the duration
 435 and strength of vertical heat fluxes associated with the late winter radiatively driven convection,
 436 and (2) the timing and duration of spring overturn dynamics (Figure 1).

437

438 The duration and strength of late-winter convection depend on the buoyancy flux from solar
 439 radiation and the depth of the surface mixed layer. In cryostratified lakes, there is strong
 440 stratification so that there is a very thin surface mixed layer. In contrast, a small increase in under
 441 ice temperatures from solar heat can potentially trigger convective mixing throughout a large
 442 region of the water column in cold cryomictic lakes that are weakly stratified (Bruesewitz et al.
 443 2015; Yang et al. 2017; Yang et al. 2020). In very large and deep lakes such as Lake Superior
 444 and Lake Michigan, the spring overturn can continue for weeks to months after ice-off, until the
 445 water column reaches 4°C (Austin, 2019; Cannon et al., 2019). Under similar meteorological
 446 forcing, we would expect that cryostratified lakes, such as Harp Lake (Figure 2b), will warm up
 447 to 4°C faster than colder cryomictic lakes after ice-off, and consequently have a shorter duration
 448 of spring overturn (Yang et al., 2020). We note that this is likely the reason that most previous
 449 studies on solar-driven convection have occurred in large deep lakes (Yang et al. 2017, 2020;
 450 Bouffard et al. 2019) rather than in smaller lakes that are typically warmer, and have only brief
 451 overturn periods (e.g. Bruesewitz et al. 2015). Similarly, the vertical velocities associated with
 452 solar-driven convection scale as $w^* \sim (Bh)^{\frac{1}{3}}$ (Kelley, 1997; Bouffard et al., 2019), where B is the
 453 buoyancy flux, and h is the depth of the surface mixed layer. It is likely that h is larger in
 454 cryomictic weakly stratified lakes during under-ice convection, and therefore these “colder”
 455 lakes are then more likely to have larger vertical velocities w^* and more vigorous convection

456 under the ice, as well as a longer duration of convection. The vigor of this convection may in
 457 turn structure the planktonic communities (Kelley, 1997; Bouffard et al., 2019) as plankton rely
 458 on the vertical circulation to remain in the photic zone (Yang et al., 2020).

459
 460 Furthermore, both the data from 19 lakes (Figure 3e) and equation (7) suggest that the
 461 temperature at ice formation may be sensitive to shifts in surface winds. In particular, ice-on
 462 temperatures in larger lakes are more sensitive to differences in surface winds as equation (7)
 463 implies that $\left| \frac{\partial T_{avg}}{\partial u_*} \right| = 8g'^{-\frac{1}{2}}A^{\frac{1}{4}}H_{max}^{-1}$ is greater for shallow lakes with larger area (see example in
 464 Figure S2). In some locations surface winds have increased by 10–20% recently (e.g. over Lake
 465 Superior, Desai et al., 2009), while in other locations winds have dropped by 10–20% (Pryor et
 466 al., 2009; Vautard et al., 2010). Such shifts in the mean surface winds or variability with late fall
 467 storm events on lakes that have ice-on temperatures that are close to 2°C might shift lakes
 468 between cryomictic and cryostratified states, depending on the surface winds.

469 470 **Limitations of the analysis**

471
 472 The main assumption we have made in our analysis is that the thermal stratification at ice-on is
 473 primarily determined by surface heat fluxes and the turbulent mixing is driven by winds. Other
 474 processes could be important in setting winter thermal stratification. For example, river inflows
 475 can impact the thermal stratification (Pasche et al., 2019; Cortés and MacIntyre, 2019), which
 476 will be important in lakes that have short residence times. The summer heat stored in the
 477 sediment can also be an important heat flux (Fang and Stefan, 1996, 1998). Finally, in very deep
 478 lakes, such as Lake Superior, compressibility effects are important, so that stable temperature
 479 profiles below 200 m follow a thermobaric relationship, rather than being a constant 4°C (Titze
 480 and Austin, 2014; Crawford and Collier, 2007; Boehrer and Schultze, 2008). This implies that
 481 the depth averaged temperature of a deep lake at ice-on might be lower than expected based on
 482 similar shallow lakes.

483 484 **Conclusions**

485
 486 Although Lewis (1983) originally classified all dimictic lakes into one group, we conclude that
 487 dimictic lakes should further be differentiated into *cryostratified* and *cryomictic*. We suggest that
 488 smaller lakes with less wind result in “warmer” under-ice temperatures near 4°C and should be
 489 termed “*cryostratified*” whereas larger lakes with higher winds are typically “colder” (near 0°C)
 490 and should be termed “*cryomictic*”. Stronger winds at the surface potentially drive a longer
 491 duration of mixing by delaying ice formation (Kirillin et al., 2012), and hence the temperature
 492 profiles at ice-on are colder and more isothermal compared to lakes with weaker winds. We
 493 developed an equation that predicts the mean temperature at ice-on from the wind speed and lake
 494 geometry (equation 7) and compares well with measurements from our study lakes. In cases
 495 where surface wind measurements are not available, the non-dimensional ratio $\log(H_{mean}/\sqrt{A})$
 496 correlates well with the mean ice-on temperature. These results suggest that there is a wide
 497 spectrum of ice-on temperature profiles in temperate, dimictic lakes. Furthermore, we expect
 498 similar processes will occur in high latitude polymictic lakes or cold monomictic lakes. For
 499 example, Lake Vörtsjärv and Shelburne Pond were two polymictic lakes included in the analysis.
 500 greater recognition and better characterization of the variability in thermal structure under the ice

501 will have important implications for understanding both the ecology and physical dynamics of
502 dimictic lakes during winter.

503

504 **Data Availability Statement**

505

506 References of all previously published data are available in Table S1 (Pierson et al. 2011; Cott et
507 al. 2015; Guzzo et al. 2016; Titze and Austin 2016; Mackay et al. 2017; Yang et al. 2017; Moras
508 et al. 2019; LSPA et al. 2020; McMeans et al. 2020; Wang et al. 2020; Yang et al. 2020).

509 Previously unpublished data are available at <http://doi.org/10.5281/zenodo.4019639>.

510

511 **Acknowledgements**

512

513 We thank the Global Lake Ecological Observatory Network for organizing the GLEON 21
514 meeting, where this work was initially conceived. BY and MGW acknowledges support from the
515 Ontario Ministry of Environment, Conservation, and Parks (Grant LS-14-15-011) and the
516 NSERC Discovery program (Grant RGPIN-2016-06542). The Lake Superior observations were
517 supported by National Science Foundation Division of Ocean Sciences grant OCE-0825633 and
518 NSF RAPID (Grant OCE-1445567). AL acknowledges support from the Estonian Research
519 Council Grant PSG32. GAW acknowledges the Swedish Infrastructure for Ecosystem Science
520 (SITES) for provisioning of data from Lake Erken. SITES receives funding through the Swedish
521 Research Council under the grant 2017-00635. Lake Mendota and Crystal Bog observations
522 were supported by the US National Science Foundation grant DEB-1440297 and grant DEB-
523 1856224. RMP acknowledges support from US National Science Foundation grants DEB
524 1754276 and DEB 1950170. CCC acknowledges support from US National Science Foundation
525 grant DEB 1753639 and 1933016. Alexie Lake data collections were supported by DeBeers
526 Canada and Fisheries & Oceans Canada

527

528

529 **References**

530

- 531 1. Austin, J. A. (2019). Observations of radiatively driven convection in a deep
532 lake. *Limnology and Oceanography*, *64*(5), 2152-2160. doi:
- 533 2. Bergstedt, R. A., Argyle, R. L., Seelye, J. G., Scribner, K. T., & Curtis, G. L. (2003). In
534 situ determination of the annual thermal habitat use by lake trout (*Salvelinus namaycush*)
535 in Lake Huron. *Journal of Great Lakes Research*, *29*, 347-361. doi:10.1016/S0380-
536 1330(03)70499-7
- 537 3. Blanchfield, P. J., Tate, L. S., Plumb, J. M., Acolas, M. L., & Beaty, K. G. (2009).
538 Seasonal habitat selection by lake trout (*Salvelinus namaycush*) in a small Canadian
539 shield lake: constraints imposed by winter conditions. *Aquatic ecology*, *43*(3), 777-787.
540 doi: 10.1007/s10452-009-9266-3

- 541 4. Block, B. D., Denfeld, B. A., Stockwell, J. D., Flaim, G., Grossart, H. P. F., Knoll, L. B.,
542 ... & Sadro, S. (2019). The unique methodological challenges of winter
543 limnology. *Limnology and Oceanography: Methods*, 17(1), 42-57.
544 doi:10.1002/lom3.10295
- 545 5. Boehrer, B., & Schultze, M. (2008). Stratification of lakes. *Reviews of Geophysics*, 46(2).
546 doi: 10.1029/2006RG000210
- 547 6. Bouffard, D., Zdrovennova, G., Bogdanov, S., Efremova, T., Lavanchy, S., Palshin, N.,
548 ... & Zdrovennov, R. (2019). Under-ice convection dynamics in a boreal lake. *Inland*
549 *Waters*, 9(2), 142-161. doi:10.1080/20442041.2018.1533356
- 550 7. Brandt, S. B., Magnuson, J. J., & Crowder, L. B. (1980). Thermal habitat partitioning by
551 fishes in Lake Michigan. *Canadian Journal of Fisheries and Aquatic Sciences*, 37(10),
552 1557-1564.
- 553 8. Bruesewitz, D. A., Carey, C. C., Richardson, D. C., & Weathers, K. C. (2015). Under-ice
554 thermal stratification dynamics of a large, deep lake revealed by high-frequency
555 data. *Limnology and Oceanography*, 60(2), 347-359. doi: 10.1005/lno.10014
- 556 9. Cannon, D. J., Troy, C. D., Liao, Q., & Bootsma, H. A. (2019). Ice-free radiative
557 convection drives spring mixing in a large lake. *Geophysical Research Letters*, 46(12),
558 6811-6820. doi: 10.1029/2019GL082916
- 559 10. Charnock, H. (1955). Wind stress on a water surface. *Quarterly Journal of the Royal*
560 *Meteorological Society*, 81(350), 639-640. doi: 10.1002/qj.49708135027
- 561 11. Chen, C. T. A., & Millero, F. J. (1986). Thermodynamic properties for natural waters
562 covering only the limnological range. *Limnology and Oceanography*, 31(3), 657-662.
563 doi: 10.4319/lo.1986.31.3.0657
- 564 12. Cortés, A., & MacIntyre, S. (2019). Mixing processes in small arctic lakes during
565 spring. *Limnology and Oceanography*. doi: 10.1002/lno.11296
- 566 13. Cote, D., Tibble, B., Curry, R. A., Peake, S., Adams, B. K., Clarke, K. D., & Perry, R.
567 (2020). Seasonal and diel patterns in activity and habitat use by brook trout (*Salvelinus*
568 *fontinalis*) in a small Newfoundland lake. *Environmental Biology of Fishes*, 103(1), 31-
569 47. doi: 10.1007/s10641-019-00931-1
- 570
- 571 14. Cott, P. A., Guzzo, M. M., Chapelsky, A. J., Milne, S. W., & Blanchfield, P. J. (2015).
572 Diel bank migration of Burbot (*Lota lota*). *Hydrobiologia*, 757(1), 3-20. doi:
573 10.1007/s10750-015-2257-6

- 574 15. Crawford, G. B., & Collier, R. W. (2007). Long-term observations of deepwater renewal
575 in Crater Lake, Oregon. *Hydrobiologia*, 574(1), 47-68. doi: 10.1007/s10750-006-0345-3
- 576 16. Crossin, G. T., Heupel, M. R., Holbrook, C. M., Hussey, N. E., Lowerre-Barbieri, S. K.,
577 Nguyen, V. M., ... & Cooke, S. J. (2017). Acoustic telemetry and fisheries
578 management. *Ecological Applications*, 27(4), 1031-1049. doi: 10.1002/eap.1533
- 579 17. Desai, A. R., Austin, J. A., Bennington, V., & McKinley, G. A. (2009). Stronger winds
580 over a large lake in response to weakening air-to-lake temperature gradient. *Nature*
581 *Geoscience*, 2(12), 855-858. doi: 10.1038/ngeo693
- 582 18. Fang, X., & Stefan, H. G. (1996). Dynamics of heat exchange between sediment and
583 water in a lake. *Water Resources Research*, 32(6), 1719-1727. doi: 10.1029/96WR00274
- 584 19. Fang, X., & Stefan, H. G. (1998). Temperature variability in lake sediments. *Water*
585 *Resources Research*, 34(4), 717-729. doi: 10.1029/97WR03517
- 586 20. Fee, E. J., Hecky, R. E., Kasian, S. E. M., & Cruikshank, D. R. (1996). Effects of lake
587 size, water clarity, and climatic variability on mixing depths in Canadian Shield
588 lakes. *Limnology and Oceanography*, 41(5), 912-920. doi: 10.4319/lo.1996.41.5.0912
- 589 21. Farmer, D. M., & Carmack, E. (1981). Wind mixing and restratification in a lake near the
590 temperature of maximum density. *Journal of physical oceanography*, 11(11), 1516-1533.
591 doi: 10.1175/1520-0485(1981)011<1516:WMARIA>2.0.CO;2
- 592 22. Gorham, E., & Boyce, F. M. (1989). Influence of lake surface area and depth upon
593 thermal stratification and the depth of the summer thermocline. *Journal of Great Lakes*
594 *Research*, 15(2), 233-245. doi: 10.1016/S0380-1330(89)71479-9
- 595 23. Gorsky, D., Zydlewski, J., & Basley, D. (2012). Characterizing seasonal habitat use and
596 diel vertical activity of lake whitefish in Clear Lake, Maine, as determined with acoustic
597 telemetry. *Transactions of the American Fisheries Society*, 141(3), 761-771.
598 doi:10.1080/00028487.2012.675905
- 599 24. Guseva, S., Bleninger, T., Jöhnk, K., Polli, B. A., Tan, Z., Thiery, W., ... & Stepanenko,
600 V. (2020). Multimodel simulation of vertical gas transfer in a temperate lake. *Hydrology*
601 *and Earth System Sciences*, 24(2), 697-715. doi: 10.5194/hess-24-697-2020
- 602 25. Guzzo, M. M., Blanchfield, P. J., Chapelsky, A. J., & Cott, P. A. (2016). Resource
603 partitioning among top-level piscivores in a sub-Arctic lake during thermal
604 stratification. *Journal of Great Lakes Research*, 42(2), 276-285. doi:
605 10.1016/j.jglr.2015.05.014

- 606 26. Hampton, S. E., Galloway, A. W., Powers, S. M., Ozersky, T., Woo, K. H., Batt, R. D., ...
607 & Stanley, E. H. (2017). Ecology under lake ice. *Ecology letters*, 20(1), 98-111. doi:
608 10.1111/ele.12699
- 609 27. Hampton, S. E., Moore, M. V., Ozersky, T., Stanley, E. H., Polashenski, C. M., &
610 Galloway, A. W. (2015). Heating up a cold subject: prospects for under-ice plankton
611 research in lakes. *Journal of plankton research*, 37(2), 277-284. doi:
612 10.1093/plankt/fbv002
- 613 28. Harrison, P. M., Gutowsky, L. F. G., Martins, E. G., Patterson, D. A., Cooke, S. J., &
614 Power, M. (2016). Temporal plasticity in thermal-habitat selection of burbot *Lota lota* a
615 diel-migrating winter-specialist. *Journal of Fish Biology*, 88(6), 2111-2129. doi:
616 10.1111/jfb.12990
- 617 29. Huey, R. B. (1991). Physiological consequences of habitat selection. *The American*
618 *Naturalist*, 137, S91-S115. doi: 10.1086/285141
- 619 30. Hsu, S. A., Meindl, E. A., & Gilhousen, D. B. (1994). Determining the power-law wind-
620 profile exponent under near-neutral stability conditions at sea. *Journal of Applied*
621 *Meteorology*, 33(6), 757-765. doi: 10.1175/1520-
622 0450(1994)033<0757:DTPLWP>2.0.CO;2
- 623 31. Kelley, D. E. (1997). Convection in ice-covered lakes: effects on algal
624 suspension. *Journal of Plankton Research*, 19(12), 1859-1880. doi:
625 10.1093/plankt/19.12.1859
- 626 32. Kirillin, G., & Shatwell, T. (2016). Generalized scaling of seasonal thermal stratification
627 in lakes. *Earth-Science Reviews*, 161, 179-190. doi: 10.1016/j.earscirev.2016.08.008
- 628 33. Kirillin, G., Leppäranta, M., Terzhevik, A., Granin, N., Bernhardt, J., Engelhardt, C., ...
629 & Zdorovenova, G. (2012). Physics of seasonally ice-covered lakes: a review. *Aquatic*
630 *sciences*, 74(4), 659-682. doi: 10.1007/s00027-012-0279-y
- 631 34. Lewis Jr, W. M. (1983). A revised classification of lakes based on mixing. *Canadian*
632 *Journal of Fisheries and Aquatic Sciences*, 40(10), 1779-1787. doi: 10.1139/f83-207
- 633 35. LSPA, K.C. Weathers, and B.G. Steele. 2020. High-Frequency Weather Data at Lake
634 Sunapee, New Hampshire, USA, 2007-2019 ver 3. Environmental Data Initiative. Doi:
635 10.6073/pasta/698e9ffb0cdcda81ecf7188bff54445e. Accessed 2020-05-14
636

- 637 36. MacKay, M. D., Versegny, D. L., Fortin, V., & Rennie, M. D. (2017). Wintertime
638 simulations of a boreal lake with the Canadian Small Lake Model. *Journal of*
639 *Hydrometeorology*, 18(8), 2143-2160. doi: 10.1175/JHM-D-16-0268.1
640
- 641 37. Markfort, C. D., Perez, A. L., Thill, J. W., Jaster, D. A., Porté-Agel, F., & Stefan, H. G.
642 (2010). Wind sheltering of a lake by a tree canopy or bluff topography. *Water Resources*
643 *Research*, 46(3). doi: 10.1029/2009WR007759
- 644 38. McMeans, B. C., McCann, K. S., Guzzo, M. M., Bartley, T. J., Bieg, C., Blanchfield, P.
645 J., ... & Ridgway, M. S. (2020). Winter in water: Differential responses and the
646 maintenance of biodiversity. *Ecology Letters*, 23(6), 922-938. doi: 10.1111/ele.13504
- 647 39. Moras, S., Ayala, A. I., & Pierson, D. (2019). Historical modelling of changes in Lake
648 Erken thermal conditions. *Hydrology and Earth System Sciences*, 23(12), 5001-5016. doi:
649 10.5194/hess-23-5001-2019
- 650 40. Mulder, I. M., Morris, C. J., Dempson, J. B., Fleming, I. A., & Power, M. (2018).
651 Overwinter thermal habitat use in lakes by anadromous Arctic char. *Canadian Journal of*
652 *Fisheries and Aquatic Sciences*, 75(12), 2343-2353. doi: 10.1139/cjfas-2017-0420
- 653 41. O'Reilly, C. M., Sharma, S., Gray, D. K., Hampton, S. E., Read, J. S., Rowley, R. J., ... &
654 Weyhenmeyer, G. A. (2015). Rapid and highly variable warming of lake surface waters
655 around the globe. *Geophysical Research Letters*, 42(24), 10773-10781. doi:
656 10.1002/2015GL066235
- 657 42. Pasche, N., Hofmann, H., Bouffard, D., Schubert, C. J., Lozovik, P. A., & Sobek, S.
658 (2019). Implications of river intrusion and convective mixing on the spatial and temporal
659 variability of under-ice CO₂. *Inland Waters*, 9(2), 162-176. doi:
660 10.1080/20442041.2019.1568073
- 661 43. Pierson, D. C., Weyhenmeyer, G. A., Arvola, L., Benson, B., Blenckner, T., Kratz, T., ...
662 & Weathers, K. (2011). An automated method to monitor lake ice phenology. *Limnology*
663 *and Oceanography: Methods*, 9(2), 74-83. doi: 10.4319/lom.2010.9.0074
- 664 44. Pryor, S. C., Barthelmie, R. J., Young, D. T., Takle, E. S., Arritt, R. W., Flory, D., ... &
665 Roads, J. (2009). Wind speed trends over the contiguous United States. *Journal of*
666 *Geophysical Research: Atmospheres*, 114(D14). doi: 10.1029/2008JD011416

- 667 45. Read, J. S., Hamilton, D. P., Desai, A. R., Rose, K. C., MacIntyre, S., Lenters, J. D., ... &
668 Rusak, J. A. (2012). Lake-size dependency of wind shear and convection as controls on
669 gas exchange. *Geophysical Research Letters*, 39(9). doi: 10.1029/2012GL051886
- 670 46. Suski, C. D., & Ridgway, M. S. (2009). Seasonal pattern of depth selection in
671 smallmouth bass. *Journal of Zoology*, 279(2), 119-128. doi: 10.1111/j.1469-
672 7998.2009.00595.x
- 673 47. Titze, D. J., & Austin, J. A. (2014). Winter thermal structure of Lake Superior. *Limnology*
674 *and oceanography*, 59(4), 1336-1348. doi: 10.4319/lo.2014.59.4.1336
- 675 48. Titze, D., & Austin, J. (2016). Novel, direct observations of ice on Lake Superior during
676 the high ice coverage of winter 2013–2014. *Journal of Great Lakes Research*, 42(5), 997-
677 1006. doi: 10.1016/j.jglr.2016.07.026
- 678 49. Wang, J., Huang, L., Ju, J., Daut, G., Ma, Q., Zhu, L., ... & Graves, K. (2020). Seasonal
679 stratification of a deep, high-altitude, dimictic lake: Nam Co, Tibetan Plateau. *Journal of*
680 *Hydrology*, 584, 124668. doi: 10.1016/j.jhydrol.2020.124668
- 681 50. Wüest, A., & Lorke, A. (2003). Small-scale hydrodynamics in lakes. *Annual Review of*
682 *fluid mechanics*, 35(1), 373-412. doi: 10.1146/annurev.fluid.35.101101.161220
- 683 51. Vautard, R., Cattiaux, J., Yiou, P., Thépaut, J. N., & Ciais, P. (2010). Northern
684 Hemisphere atmospheric stilling partly attributed to an increase in surface
685 roughness. *Nature geoscience*, 3(11), 756-761. doi: 10.1038/ngeo979
- 686 52. Verpoorter, C., Kutser, T., Seekell, D. A., & Tranvik, L. J. (2014). A global inventory of
687 lakes based on high-resolution satellite imagery. *Geophysical Research Letters*, 41(18),
688 6396-6402. doi: 10.1002/2014GL060641
- 689 53. Wetzel, R. G. (2001). *Limnology: lake and river ecosystems*. gulf professional
690 publishing.
- 691 54. Yang, B., Young, J., Brown, L., & Wells, M. (2017). High-frequency observations of
692 temperature and dissolved oxygen reveal under-ice convection in a large
693 lake. *Geophysical Research Letters*, 44(24), 12218-12226. doi: 10.1002/2017GL075373
- 694 55. Yang, B., Wells, M. G., Li, J., & Young, J. (2020). Mixing, stratification, and plankton
695 under lake-ice during winter in a large lake: Implications for spring dissolved oxygen
696 levels. *Limnology and Oceanography*. doi: 10.1002/lno.11543

